

Eq. (A5)]:

$$\partial_{AB'}\psi^{ACDE}=0. \quad (\text{A8})$$

The Penrose function for gravitational field is

$$\psi \equiv \psi_{ABCD}\xi^A\xi^B\xi^C\xi^D. \quad (\text{A9})$$

Knowledge of ψ on a null cone provides a unique, independent, nonredundant characterization of solutions of the Einstein equations.

The vector field $C^\rho(r)$ of Eq. (2) can be expressed in spinor notation by means of the Hermitian spinor

$$C^{AF'} = \psi^{ABCD}\partial_{B'}r_{CD} + \psi^{F'B'C'D'}\partial_{B'}r_{C'D'}, \quad (\text{A10})$$

where r_{CD} is the symmetric spinor associated with the arbitrary bivector $r_{\mu\nu}$ by means of Eq. (A2). It is easily confirmed that

$$\partial_{AB'}C^{AB'}=0. \quad (\text{A11})$$

Determination of π - π Cross Sections by the Chew-Low Extrapolation Method*

D. DUANE CARMONY† AND REMY T. VAN DE WALLE‡

Lawrence Radiation Laboratory, University of California, Berkeley, California

(Received March 15, 1962)

A discussion of the Chew-Low conjecture applied to reactions of the type $\pi+p \rightarrow \pi+p+\pi^0$ is given. The extrapolation technique and the so-called "physical-region-plot method" are discussed. These methods are then applied to a sample of 1684 interactions of the type $\pi^++p \rightarrow \pi^++p+\pi^0$ and 411 interactions of the type $\pi^-+p \rightarrow \pi^-+p+\pi^0$ at 1.25-BeV/c incident pion momentum. In Sec. II, we present details of the way in which this sample was obtained and processed. The $\sigma_{\pi^+\pi^0}$ physical-region plots for the π^+ data confirm the existence of the now well-established $T=J=1$ π - π resonance at 725 ± 25 MeV. On the other hand, the physical-region plot of the π^- data shows strong deviations from the results expected on the basis of this same resonance.

Extrapolation results are presented in detail for seven different π - π energy regions. The π^- and π^+ data (although very different in the physical region) extrapolate to the same π - π cross-section values for energy regions around the resonance. This fact and the general character of the π^- extrapolations indicate that the π^- physical-region distortions should be attributed to final-state interactions. Although the errors are large, the π - π cross-section curve obtained by extrapolation on the combined $\pi^+\pi^-$ sample, is in full agreement with the existence of a π - π P -wave resonance at 725 ± 25 MeV.

I. THE CHEW-LOW CONJECTURE

DURING the past few years—mainly under the impulse of the dispersion-relation development—a considerable amount of study has been devoted to detecting the presence and the location of singularities in S matrices. In most cases, the existence and the location of these singularities was actually conjectured on the basis of plausibility arguments supplied by perturbation calculations using conventional field theory; in some special instances, proofs were given.

Singularities in the momentum-transfer variables have been utilized for practical purposes following a proposal by Chew¹ to determine the pion-nucleon coupling constant from either nucleon-nucleon scattering data² or photoproduction data.³ Using the same principles (actually, generalizing them), Chew and Low made

a conjecture opening the possibility of determining cross sections on targets not available in the laboratory.⁴ The conjecture states that:

a. Each S -matrix element corresponding to a definite number of particles (when considered as a function of the independent invariants of the problem) has poles at points related to the masses of the single-particle states which can occur as intermediate states between two subgroups of particles formed from the total group.

b. The residue of such an S -matrix pole is given by the product of two (dimensionally smaller) S -matrix elements, each of which connects a subgroup to the intermediate particle. These submatrix elements can correspond to processes not realizable in the laboratory. They now become "measurable" by means of a residue evaluation of the over-all S -matrix element at the pole in question. Since the poles discussed here lie in regions of the variables that are not physically allowed, this residue evaluation is connected with extrapolation procedures.

The Chew-Low conjecture, stated specifically with respect to the poles in the *momentum-transfer variable*, has been used in an "orthodox" way (i.e., by actually

* This work was done under the auspices of the U. S. Atomic Energy Commission.

† Partially based on work submitted to the graduate division of the University of California in partial fulfillment of the requirements for the degree of Doctor of Philosophy.

‡ On leave of absence from the Inter-University Institute for Nuclear Sciences, Brussels, Belgium.

¹ Geoffrey F. Chew, Phys. Rev. **112**, 1380 (1958).

² P. Cziifra and M. J. Moravcsik, Phys. Rev. **116**, 226 (1959).

³ J. G. Taylor, M. J. Moravcsik, and J. L. Uretsky, Phys. Rev. **113**, 689 (1959).

⁴ G. F. Chew and F. E. Low, Phys. Rev. **113**, 1640 (1959).

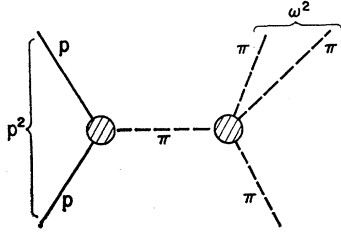


FIG. 1. Pole diagram for the single-pion production process.

performing the extrapolations implied by it) by a number of physicists. Swanson *et al.*, used it to determine total cross sections for the process $\gamma+n \rightarrow \pi^-+p$ from their $\gamma+d \rightarrow p+\pi^-$ data.⁵ Smith *et al.*, in an effort to test the validity of the Chew-Low conjecture, analyzed their $p+p \rightarrow p+n+\pi^+$ data and were able to reproduce average π^+-p cross sections in agreement with the $\frac{3}{2}, \frac{3}{2}$ resonance.⁶ Anderson *et al.* used the Chew-Low method to determine the $\pi-\pi$ cross sections from their single- π^0 -production data.⁷⁻⁹

All these analyses generally agree with the predictions of the Chew-Low conjecture but do not allow detailed conclusions for reasons that can always be attributed to the large amount of statistics needed to make the required extrapolations in a meaningful way.

Specifically, when applied to the reaction

$$\pi+p \rightarrow \pi+p+\pi^0, \quad (1)$$

the Chew-Low conjecture refers to the diagram shown in Fig. 1, where p is the four-momentum transfer to the proton, and ω is the total energy of the two final-state pions in their own c.m. frame. In terms of laboratory quantities, these two invariants are defined¹⁰ as

$$p^2 = 2MT = P_p^2 - [M - (M^2 + P_p^2)^{1/2}]^2 \quad (2)$$

and

$$\omega^2 = [(q^2 + \mu^2)^{1/2} - T]^2 - (q^2 - 2qP_p \cos\theta_{\text{lab}} + P_p^2),$$

where T and P_p are, respectively, the kinetic energy and momentum of the recoiling proton in the laboratory system, M is the proton mass, q is the beam momentum, μ is the pion mass, and θ_{lab} is the laboratory angle between the incident pion and the recoiling proton.

According to the Chew-Low conjecture, the matrix element for process (1) has a pole at $p^2 = -\mu^2$, with a residue given by $fA_{\pi\pi}(\omega^2)$, where f is the renormalized pion-nucleon coupling constant ($f^2 \approx 0.08$) and $A_{\pi\pi}$ is the pion-pion scattering amplitude. More precisely,

⁵ W. P. Swanson, D. C. Gates, T. L. Jenkins, and R. W. Kenney, *Phys. Rev. Letters* **5**, 339 (1960).

⁶ G. A. Smith, H. Courant, E. Fowler, H. Kraybill, J. Sandness, and H. Taft, *Phys. Rev. Letters* **5**, 571 (1960).

⁷ J. A. Anderson, V. X. Bang, P. G. Burke, D. D. Carmony, and N. Schmitz, *Phys. Rev. Letters* **6**, 365 (1961).

⁸ J. A. Anderson, V. X. Bang, P. G. Burke, D. D. Carmony, and N. Schmitz, *Revs. Modern Phys.* **33**, 431 (1961).

⁹ Norbert Schmitz, thesis, University of Munich, Germany, 1961 (unpublished).

and in terms of cross sections, the statement says that

$$\frac{\partial^2 \sigma}{\partial p^2 \partial \omega^2} \xrightarrow{p^2 \rightarrow -\mu^2} \frac{f^2}{2\pi} \frac{p^2/\mu^2}{(p^2 + \mu^2)^2} \frac{F(\omega^2)}{q^2} \sigma_{\pi\pi}(\omega^2), \quad (3)$$

in which $\partial^2 \sigma / \partial p^2 \partial \omega^2$ and $\sigma_{\pi\pi}$, respectively, represent the differential cross section for process (1) and the total cross section for the process

$$\pi + \pi \rightarrow \pi + \pi, \quad (4)$$

and $F(\omega^2)$ is a kinematical factor given by $[\omega^2(\omega^2/4 - \mu^2)]^{1/2}$; the other symbols have the same meaning as above.

A straightforward procedure for obtaining information about the residue consists of fitting the distribution

$$G(p^2, \omega^2) = (p^2 + \mu^2)^2 (\partial^2 \sigma / \partial p^2 \partial \omega^2) q^2 / F(\omega^2) (2\pi / f^2) \quad (5)$$

with a polynomial of the form⁸

$$A_0 + A_1(p^2 + \mu^2) + A_2(p^2 + \mu^2)^2 + \dots \quad (6)$$

for each ω^2 region under consideration.

Then we have

$$\sigma_{\pi\pi}(\omega^2) = -A_0. \quad (7)$$

It follows from relation (3) that if only the pole term influences the physical region, expression (6) should reduce to

$$A_0 - A_0(p^2 + \mu^2)/\mu^2. \quad (8)$$

In other words, under these circumstances, distribution (5) considered as a function of p^2 would be fitted by a straight line going through the origin. In general, however, contributions due to three, or more, pion intermediate states will tend to destroy this behavior.

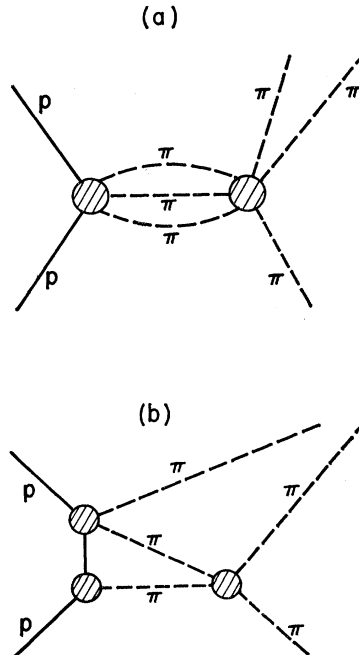


FIG. 2. (a) General branch-cut diagram and (b) final-state interaction diagram for the single-pion production process.

In their most general form, the three-pion contributions can be represented by the diagram shown in Fig. 2(a). This is termed a "branch-cut" contribution because it corresponds to a branch-cut singularity of the S matrix lying on the real p^2 axis, extending from $-9\mu^2$ to $-\infty$.

A special example of these branch-cut contributions is the final-state interaction, schematically represented in Fig. 2(b). Data influenced by the "branch-cut" require higher-order polynomial fits.

To obtain data that *a priori* may be dominantly influenced by the pole contribution, one should limit the analysis to events that are near that pole, i.e., events characterized by a low-momentum transfer to the proton. This limitation is also evident on direct physical grounds, as low-momentum-transfer events are interactions where the incoming pion has collided with a large impact parameter, i.e., has most likely interacted with pions of the nucleon cloud, and not directly with the nucleon core. Furthermore, within the framework of pion-cloud collisions, impact parameters larger than the Yukawa range of the three-pion exchange processes will minimize contributions from the branch cut.

The Chew-Low conjecture applied to reaction (1) has also been frequently used without actually performing the extrapolations implied by it. In this case, one assumes that relation (3) is a correct representation of the single- π^0 -production matrix element, not only at the pole $p^2 = -\mu^2$, but also over the beginning of the physical p^2 region.¹⁰ The latter assumption can then be exploited in two different ways: It can be used to derive the momentum spectrum of the recoil protons by performing an integration over ω^2 [assuming a certain $\sigma_{\pi\pi}(\omega^2)$ vs ω^2 dependence], or else it can be used to make so-called "physical region cross section" plots of $\sigma_{\pi\pi}(\omega^2)$ vs ω^2 . In the latter procedure one actually plots

$$\sigma_{\pi\pi}(\omega^2) = \frac{2\pi}{f^2} \frac{q^2}{F(\omega^2)} \left\langle \frac{(p^2 + \mu^2)^2}{p^2/\mu^2} \frac{\partial^2 \sigma}{\partial p^2 \partial \omega^2} \right\rangle \quad (9)$$

The angular brackets indicate an average over the region $p_{\min}^2 \leq p^2 \leq p_{\max}^2$, p_{\min}^2 being a lower kinematical limit for p^2 in the ω^2 region under consideration, and p_{\max}^2 the value of p^2 which limits the low-momentum transfer region under investigation. The "physical-region plots" as described above are actually nothing more than special Q -value plots. The Chew-Low conjecture now serves only to relate the ordinate of these Q -value plots to a $\pi-\pi$ cross section. In this paper we will discuss the application of the Chew-Low method to a sample of single π^0 production events obtained by means of a π beam of momentum 1.25 BeV/c.

¹⁰ E. Pickup, D. K. Robinson, and E. O. Salant, Phys. Rev. Letters 7, 192 (1961); A. R. Erwin, R. March, W. D. Walker, and E. West, *ibid.* 6, 628 (1961). See also the bibliographies of these works.

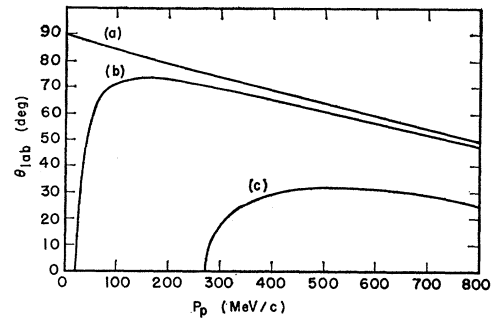


FIG. 3. Kinematics at 1255 MeV/c. Curve (a) shows the relationship between the laboratory space angle and momentum of the proton in the elastic reaction $\pi+p \rightarrow \pi+p$. Curve (b) bounds the allowed region for the reaction $\pi+p \rightarrow p+\pi+\pi^0$. Curve (c) shows the relationship between θ_{lab} and P_p for the reaction $\pi+p \rightarrow p+\rho$, where the mass of the ρ is 725 MeV.

II. EXPERIMENTAL DETAILS

The pion-pion interaction was investigated by means of the reactions

$$\pi^\pm + p \rightarrow \pi^\pm + p + \pi^0 \quad (10)$$

at the Lawrence Radiation Laboratory by using the 72-in. hydrogen bubble chamber and a 1.25-BeV/c π^\pm beam designed by Professor F. Crawford, Jr. The experiment consisted of looking for two-prong events with a stopping secondary proton of ≤ 60 -cm range and an interaction point lying within a fiducial volume.

As discussed in Sec. I, the restriction to low-momentum transfer events is indicated by the physical ideas underlying the experiment. It further has the very useful feature that for these events a very large fraction of the more frequent elastic events $\pi^\pm + p \rightarrow \pi^\pm + p$ can be eliminated from the sample by means of relatively crude scan-table measurement of the range (R) of the recoiling proton and the space angle (θ_{lab}). Figure 3, showing kinematical relations between θ_{lab} and P_p for both the elastic and the single- π^0 production events, illustrates this statement.

To avoid biases, we did not accept interactions associated with protons of less than 2.5-mm range (≤ 95 -MeV/c momentum). The single-scan efficiency was 85%. The π^- film was scanned once; the π^+ film twice. Path lengths were determined by track counting on every twentieth frame. Both the π^+ and π^- path lengths were corrected for a 3% lepton contamination; the π^+ path length was also corrected for a 2% proton contamination.

The beam momentum was calibrated by comparing radii measurements both of our beam tracks and also of previously obtained 1.03-BeV/c π^\pm film and by using the Σ - K threshold as a standard.¹¹ The mean beam momentum in the middle of the chamber was found to be 1255 ± 6 MeV/c. The kinematically allowed $p^2 - \omega^2$

¹¹ D. D. Carmony and R. T. Van de Walle, Lawrence Radiation Laboratory Alvarez Group Memorandum No. 351, 1961 (unpublished).

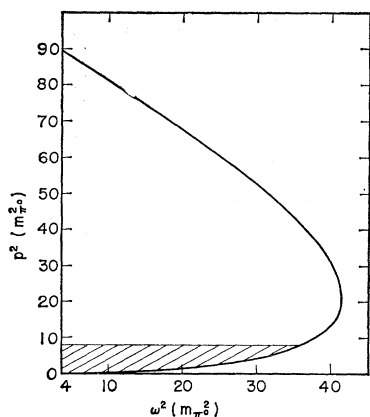


FIG. 4. Kinematically allowed region, p^2 vs ω^2 , for an incident beam momentum of 1255 MeV/c.

region for this incident beam momentum is shown in Fig. 4.

All candidate events were measured on the Franckenstein, a high-precision, bubble-chamber film-measuring device. They were geometrically reconstructed with the help of the PANG computer program and kinematically interpreted with the aid of the KICK program. The KICK output was then processed by a series of programs of the so-called EXAMIN type. Among other things, these programs make the following tests:

a. They test whether the errors on the various important quantities are within demanded tolerances, e.g., the error on the missing mass as computed by KICK is for a normal event of the order of $m_\pi/10$. An event with a computed error in the missing mass several times larger than $m_\pi/10$ was considered to be *mismeasured* and therefore was remeasured. This allowed us to keep a meaningful separation between the reactions

$$\pi + p \rightarrow \pi + p, \quad \pi + p \rightarrow \pi + p + \pi^0,$$

and

$$\pi + p \rightarrow \pi + p + \pi^0 + \pi^0$$

on the basis of the missing mass.

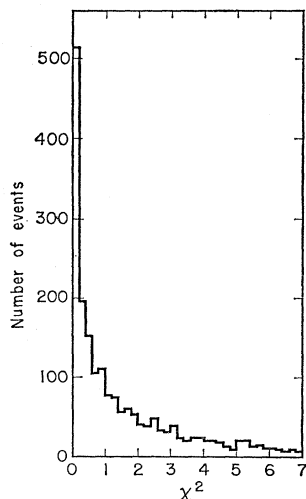


FIG. 5. The χ^2 distribution for 1915 single- π^0 -production events.

b. The EXAMIN programs test whether the measured beam momentum is within 50 MeV/c of the nominal beam momentum. Although the calculation of the histogram quantities ω^2 and p^2 is actually performed with the individually fitted beam momenta, some restriction on the accepted beam momenta is required for several reasons. First, both the pole and the branch-cut distribution depend on the beam momentum q , and when performing extrapolations, one tacitly assumes that this q is identical for all events. Second, one has to keep negligible any variations in corrections, which were calculated with the nominal beam momentum.

c. The EXAMIN programs test whether or not the reaction is an event of type (10) by using the missing mass and both the absolute and the relative magnitudes of the χ^2 values for the elastic and the single- π^0 -production hypothesis. The χ^2 distribution of 1915 of our interactions identified as single- π^0 -production events is shown in Fig. 5. This χ^2 distribution is too wide, with respect to that expected for one degree of freedom, by a scale factor of about 1.5. This implies that our input errors are too small by a factor of $\sqrt{1.5}$. We rejected all events for which $\chi^2/1.5$ was below the 1% probability level.

In Fig. 6 we show a representative missing-mass distribution based on 1500 of our inelastic interactions. About 15% of these inelastic events are multi- π^0 productions. (As can be seen from Fig. 6, only a small fraction of the inelastic events are ambiguous.)

For the accepted single-production events, the EXAMIN programs: (a) calculate the invariants ω^2 and p^2 , (b) assign an escape-correction factor (see below), and (c) collect the events into two-dimensional $G(\omega^2, p^2)$ histograms [cf. Eq. (5)]. By escape corrections we mean a weighing factor given to each event belonging to a specific ω^2 - p^2 box, to compensate for the fact that a certain fraction of the events belonging to that same box will not be "observed," as they are so oriented in the chamber that the recoiling proton leaves the fiducial volume. These correction factors were computed by means of a computer program (COR) in the following manner¹²:

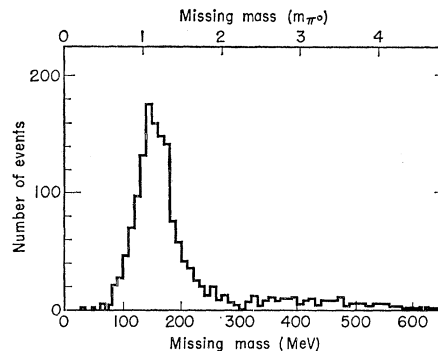


FIG. 6. Missing-mass distribution for 1500 inelastic events.

¹² Norbert Schmitz, Lawrence Radiation Laboratory Alvarez Group Memorandum No. 211, 1960 (unpublished).

For each histogram box ω^2-p^2 , or equivalently for each corresponding pair of values R, θ_{lab} of the recoiling proton, an ensemble of potential interaction points was chosen. These interaction points were distributed over the fiducial volume according to the experimentally determined beam distribution. At each of these interaction points, and in the known beam direction, a cone was constructed of side R and opening angle θ_{lab} . For $R > 20$ cm we took into account the proton curvature. The program then calculated what fraction of the cone base circumference lies outside the fiducial volume and, averaging over the ensemble of interaction points, deduced from this the total fraction of events of this category which must have "escaped" from our sampling. Table I shows a set of correction factors used for our π^+ film. Finally, a correction was made to those $p^2-\omega^2$ histogram boxes that are not entirely allowed on kinematical grounds (i.e., those intersected by the curve shown in Fig. 4).

III. RESULTS AND CONCLUSIONS

Using the methods described above, we obtained a final sample of low-momentum-transfer events with a proton momentum ≤ 400 MeV/c (i.e., $R \leq 60$ cm). We collected 1684 events of the type

$$\pi^+ + p \rightarrow \pi^+ + p + \pi^0,$$

and 411 events of the type

$$\pi^- + p \rightarrow \pi^- + p + \pi^0.$$

In Fig. 7 we show the physical-region plots for these two groups of data. The π^+ data confirm the existence of the previously observed $\pi-\pi$ resonance (or ρ meson) at $\omega^2 \approx 29 m_{\pi^0}^2$ (or $\omega = 725 \pm 25$ MeV).¹⁰ In a preceding article,¹³ we gave $\pi^+-\pi^0$ angular distributions deduced from this same π^+ sample, which formed direct evidence that the 725-MeV resonance is a $J=1$ (and hence $T=1$) resonance. The total cross-section resonance peak has a height of roughly 70% of the one expected on the basis of an elastic $J=1$ resonance. This difference can be considered as normal if one realizes that these cross sections are actually determined off the

TABLE I. Escape correction factors (π^+).

ω^2 ($m_{\pi^0}^2$)	p^2 ($m_{\pi^0}^2$)							
	1	2	3	4	5	6	7	8
7	1.003	1.018	1.043	1.127	1.361
11	1.001	1.013	1.040	1.109	1.430
15	1.000	1.011	1.038	1.114	1.311	1.616
21	...	1.007	1.032	1.089	1.171	1.509
25	...	1.004	1.003	1.069	1.138	1.284	1.781	...
29	1.055	1.097	1.191	1.385	...
31	1.100	1.154	1.287	1.677
35	1.150	1.232	1.343

¹³ D. D. Carmony and R. T. Van de Walle, Phys. Rev. Letters 8, 73 (1962); D. D. Carmony, thesis, Lawrence Radiation Laboratory Report UCRL-9886, 1961 (unpublished).

energy shell and that there could very well be some inelastic contributions at these energies.

Although suggestive in their structure, the π^- data show, in the smallness of the observed cross section, strong deviations from the results that one would expect on the basis of a $J=1$ resonance at the energy indicated by the π^+ data.

Recently an analogous experiment was done at this laboratory at an incident pion momentum of 1.03 BeV/c, resulting in a sample of mainly $\pi^- + p \rightarrow \pi^- + p + \pi^0$ data.^{7,8} The physical-region plots of this experiment showed a quasi-flat $\sigma_{\pi\pi}(\omega^2)$ curve of the order of 30 mb, i.e., gave also cross-section values smaller than the ones predicted for a $J=1$ resonance.

In Fig. 8 we show the $G(\omega^2, p^2)$ histograms of the combined $\pi^+\pi^-$ data and the linear extrapolations performed on them for six different ω^2 regions. In Table II we show the extrapolation results and the χ^2 values for both linear and quadratic fits. From this table it can be seen that a linear fit is adequate for all histograms. The end of the physically allowed region is marked on each graph as an extended heavy line on the p^2 axis.

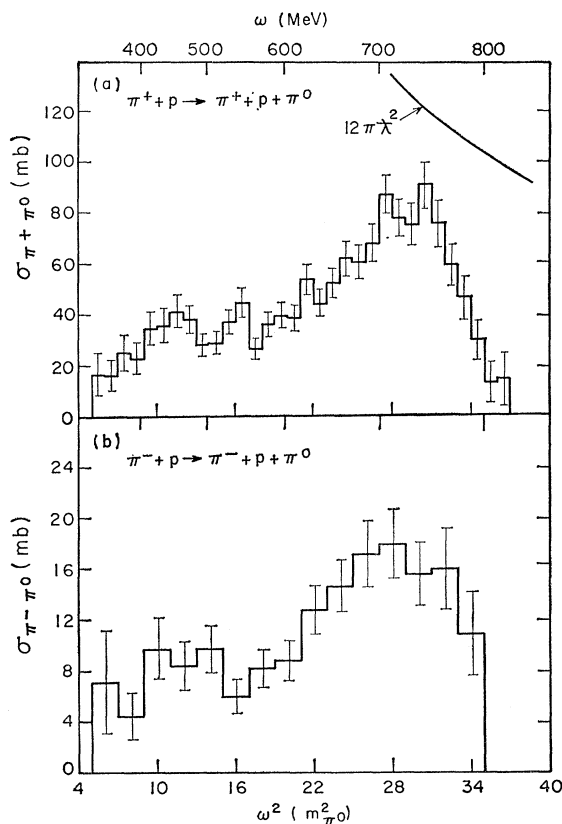


FIG. 7. (a) The total pion-pion cross section determined in the physical region from the reaction $\pi^+ + p \rightarrow p + \pi^+ + \pi^0$ as a function of the square of the di-pion total energy [Eq. (9)]. (b) The total pion-pion cross section determined in the physical region from the reaction $\pi^- + p \rightarrow p + \pi^- + \pi^0$ as a function of the square of the di-pion total energy [Eq. (9)].

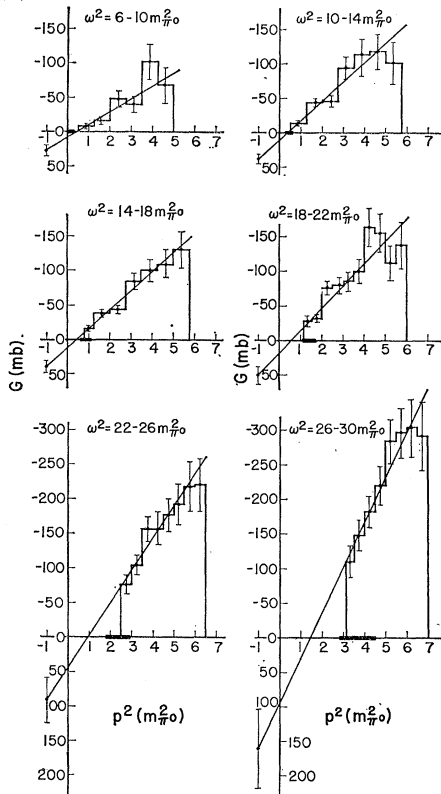


FIG. 8. Extrapolation plots and least-squares fitted curves for the combined data, $\pi^+ + p \rightarrow p + \pi^+ + \pi^0$ and $\pi^- + p \rightarrow p + \pi^- + \pi^0$.

None of the linear fits was constrained to stay positive in the physical region.

The π^- and π^+ data were also extrapolated separately. In the resonance region (i.e., for $\omega^2 \geq 20 m_{\pi^0}^2$), the π^+ and π^- data gave extrapolated $\sigma_{\pi\pi}$ values in agreement with each other within the error limits. This is illustrated in Fig. 9, which shows the π^+ and π^- extrapolations for the region $22 m_{\pi^0}^2 \leq \omega^2 \leq 26 m_{\pi^0}^2$. Below the resonance region (outside the influence of the pole), the extrapolated $\pi^-\pi^0$ cross sections kept more the character of the physical region, i.e., tended to be somewhat smaller

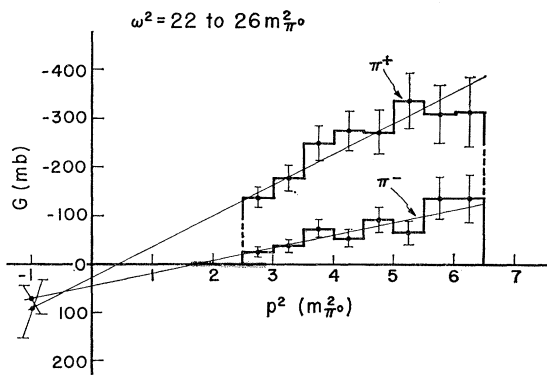


FIG. 9. Comparison of the π^+ and π^- extrapolation plots and fitted curves in the region $\omega^2 = (22 \text{ to } 26)m_{\pi^0}^2$.

TABLE II. Extrapolation results.

ω^2 region ($m_{\pi^0}^2$)	Type of fit	$\sigma_{\pi\pi}$	$\Delta\sigma_{\pi\pi}$	χ^2	Degrees of freedom	Probability level (%)
6 to 10	linear	27	8	4.6	4	34
	quadratic	19	28	4.5	3	21
10 to 14	linear	38	7	6.2	5	29
	quadratic	58	23	5.3	4	26
14 to 18	linear	39	8	3.2	5	67
	quadratic	42	26	3.2	4	52
18 to 22	linear	51	13	13.9	9	13
	quadratic	129	46	10.8	8	22
22 to 26	linear	92	33	2.6	6	86
	quadratic	313	188	1.2	5	95
26 to 30	linear	161	57	3.0	6	80
	quadratic	616	336	1.3	5	93
30 to 34	linear	-153	181	0.9	4	92
	quadratic	-2000	2000	1.0	3	80

than the corresponding $\pi^+ - \pi^0$ values. Figure 9 also shows another general feature of the π^+ and π^- extrapolation curves: The π^+ linear fit cuts the p^2 axis near the origin, indicating a dominance of the pole term in the physical region, while the π^- fitted line has a much larger p^2 intercept, thus indicating a much stronger contribution of the branch cut in the physical region. These conclusions agree with the experimental results mentioned above.^{7,8} They also support the interpretation that our π^- data distortions are due to final-state interactions. In spite of this stronger branch-cut contribution, the π^- data remain fitted by a straight line. This can be understood in terms of the fact that the branch cut contributes mainly through its interference with the pole term. On the other hand, statistical limitations make the detection of small quadratic terms impossible.

The $\sigma_{\pi\pi}(\omega^2)$ curve obtained through extrapolation of the combined π^\pm data is shown in Fig. 10. As for the physical-region plots, a $12\pi\lambda^2$ curve is given to show the compatibility with the existence of a $J=1$ resonance. The cross sections obtained, although they

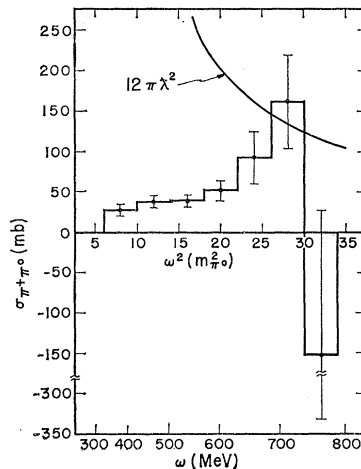


FIG. 10. The total elastic pion-pion cross section determined by extrapolation as a function of the square of the dipion total energy.

have large errors, are in complete agreement with the physical-region plots obtained by other authors¹⁰ as well as our own [Fig. 7(a)].

The results given here support the general validity of the Chew-Low technique. They illustrate the strong statistical requirements to which a meaningful application of this technique is subjected; they also show that pole effects seen in the physical region are confirmed by extrapolation, as required. The reverse, however, is not necessarily true: pole contributions obtained correctly through extrapolations can be washed out in the physical region by contributions other than those of poles. Extrapolation results are therefore to be used in parallel with physical-region plots. Physical-region plots, which require less statistics than do extrapolations in order to be meaningful, are more useful therefore in detecting the location, width, etc. of the eventual resonance.

Extrapolation results then give additional weight to these conclusions and provide the ultimate proof that the production process was indeed a peripheral one.

ACKNOWLEDGMENTS

It is a pleasure to thank Professor Luis W. Alvarez for his great interest in this experiment and Professor G. F. Chew for many helpful discussions. We are indebted to Professor Frank Crawford, Jr., who designed the beam, as well as to Professor Arthur H. Rosenfeld, Professor Lynn Stevenson, Professor George H. Trilling, Dr. John L. Brown, and Dr. Philip G. Burke for interesting and stimulating discussions.

One of us (R. V. d. W.) would like to express his gratitude to the Inter-University Institute for Nuclear Sciences (Brussels, Belgium) for making his stay at the Lawrence Radiation Laboratory possible.

Broken Symmetries*

JEFFREY GOLDSTONE

Trinity College, Cambridge University, Cambridge, England

AND

ABDUS SALAM AND STEVEN WEINBERG†

Imperial College of Science and Technology, London, England

(Received March 16, 1962)

Some proofs are presented of Goldstone's conjecture, that if there is continuous symmetry transformation under which the Lagrangian is invariant, then either the vacuum state is also invariant under the transformation, or there must exist spinless particles of zero mass.

I. INTRODUCTION

IN the past few years several authors have developed an idea which might offer hope of understanding the broken symmetries that seem to be characteristic of elementary particle physics. Perhaps the fundamental Lagrangian is invariant under all symmetries, but the vacuum state¹ is not. It would then be impossible to prove the usual sort of symmetry relations among S -matrix elements, but enough symmetry might remain (perhaps at high energy) to be interesting.

But whenever this idea has been applied to specific models, there has appeared an intractable difficulty. For example, Nambu suggested that the Lagrangian might be invariant under a continuous chirality transformation $\psi \rightarrow \exp(i\theta \cdot \tau \gamma_5) \psi$ even if the fermion physical mass M were nonzero. But then there would

be a conserved current J_λ , with matrix element

$$\langle p' | J_\lambda | p \rangle = f(q^2) \bar{u}' \gamma_5 [i \gamma_\lambda - (2M/q^2) q_\lambda] u,$$

where $q = p - p'$. The pole at $q^2 = 0$ can only arise from a spinless particle of mass zero, which almost certainly does not exist. Of course, the pole would not occur if $f(0) = 0$, which might be the case if we do not insist on identifying J_λ with the axial vector current of β decay. But Nambu showed that this unwanted massless "pion" also appears as a solution of the approximate Bethe-Salpeter equation.¹

Goldstone² has examined another model, in which the manifestation of "broken" symmetry was the nonzero vacuum expectation value of a boson field. (This was suggested as an explanation of the $\Delta I = \frac{1}{2}$ rule by Salam and Ward.)³ Here again there appeared a spinless particle of zero mass. Goldstone was led to conjecture that this will always happen whenever a continuous symmetry group leaves the Lagrangian but not the vacuum invariant.

* This research was supported in part by the U. S. Air Force under a contract monitored by the Air Force Office of Scientific Research of the Air Development Command and the Office of Naval Research.

† Alfred P. Sloan Foundation Fellow; Permanent address: University of California, Berkeley, California.

¹ Y. Nambu and G. Jona-Lasinio, Phys. Rev. **122**, 345 (1961); W. Heisenberg, Z. Naturforsch. **14**, 441 (1959).

² J. Goldstone, Nuovo cimento **19**, 154 (1961).

³ A. Salam and J. C. Ward, Phys. Rev. Letters **5**, 512 (1960).